Journal of Mammalian Evolution (2020) 27:1–16
https://doi.org/10.1007/s10914-018-9451-z

ORIGINAL PAPER

New Specimens of the Late Cretaceous Metatherian *Eodelphis* and the Evolution of Hard-Object Feeding in the Stagodontidae

Alexandria L. Brannick[1] · Gregory P. Wilson[1,2]

Published online: 29 September 2018

Abstract

The Stagodontidae include the largest metatherians known from the Cretaceous of North America. Of the recognized species of the stagodontid genus *Eodelphis*, *E. cutleri* is larger and has a more robust dentary, more inflated premolars, and third premolars specialized for crushing, as opposed to the more gracile *E. browni*. These differences have led to the hypothesis that an *E. cutleri*-like ancestor gave rise to *Didelphodon*—another, mostly younger, stagodontid, which has been interpreted as a durophagous predator-scavenger. If correct, *E. cutleri* would be expected to show more morphological adaptation toward durophagy than *E. browni* does. Here, we describe two new dentary fossils referable to *E. browni* and test the evolutionary hypothesis by applying beam theory to estimate bending force capabilities of 22 dentaries of Cretaceous stagodontids and other metatherians. The resulting diversity of bending force profiles of the sampled dentaries implies that Cretaceous metatherians had a wide range of feeding behaviors. Among the stagodontids, *E. cutleri* has a mediolateral bending force profile of the dentary that is more similar to that of *Didelphodon* than it is to that of *E. browni*; whereas its dorsoventral bending force profile is more similar to that of *E. browni*. These results indicate that anteriorly the dentary of *E. cutleri* was capable of resisting high torsional stresses from hard-object feeding but lacked other dorsoventral buttressing associated with exceptionally high bite forces of *Didelphodon*. Our results imply that some morphological changes associated with durophagy evolved twice within this clade, independently in *E. cutleri* and *Didelphodon*.

Keywords Stagodontidae · Beam theory · Durophagy · Metatheria · Cretaceous

Introduction

The Metatheria, the stem-based clade of living marsupials and their closest relatives (Rougier et al. 1998), achieved substantial taxonomic and morphological diversity during the Late Cretaceous (ca. 100–66 million years ago [Ma]; Kielan-Jaworowska et al. 2004; Sánchez-Villagra 2013; Williamson et al. 2014; Wilson et al. 2016). Yet, surprisingly few studies have quantitatively investigated the paleoecologies implied by that diversity (Clemens 1966; Luo 2007; Wilson 2013; Grossnickle and Polly 2013; Wilson et al. 2016; Grossnickle and Newham 2016). In general, because of the preservational bias toward teeth in the mammalian fossil record, studies of the paleoecology of Mesozoic mammals have primarily focused on reconstructions of diets based on dental shape and functional morphology (e.g., Crompton and Kielan-Jaworowska 1978; Jernvall et al. 1996; Wilson et al. 2012). Analysis of the dentary can also be used in functional morphological studies to infer feeding behaviors in both extant and extinct mammals (Biknevicius and Ruff 1992a, b; Grossnickle and Polly 2013; Gill et al. 2014; Grossnickle 2017). For example, cross-sectional properties of the dentary, including cortical bone structure, reflect the biomechanical bending strength of the dentary and can help constrain dietary inferences (e.g., Therrien 2005; Binder et al. 2016; Wilson et al. 2016).

In this study, we quantify biomechanical properties of the dentary in the metatherian clade Stagodontidae, which

Electronic supplementary material The online version of this article (https://doi.org/10.1007/s10914-018-9451-z) contains supplementary material, which is available to authorized users.

✉ Alexandria L. Brannick
brannick@uw.edu

[1] Department of Biology, University of Washington, Seattle, Washington, DC 98195-1800, USA

[2] Burke Museum of Natural History and Culture, Seattle, Washington, DC 98195-1800, USA

includes some of the largest bodied mammals known from the Cretaceous of North America (body mass estimate of *Didelphodon vorax* UWBM 94084 = 5.2 kg; Wilson et al. 2016). The genera *Eodelphis* and *Didelphodon* are included in this clade, in addition to the recently described genera *Fumodelphodon* and *Hoodootherium* from the Straight Cliffs Formation of Utah (Cohen 2017); a fifth genus, *Pariadens*, has also been considered a basal stagodontid (Cifelli and Eaton 1987; Rougier et al. 2004, 2015; Wilson et al. 2016; Cohen 2017; but see Fox and Naylor 2006; Williamson et al. 2012, 2014). Furthermore, the Eocene genus *Eobrasilia* of South America most recently has been proposed as a sister taxon to *Didelphodon* (Carneiro and Oliveira 2017). In addition to larger body size, stagodontids are characterized by several dental characters, including: (1) upper molars with a robust metacone, a small paracone, well-developed conules near the paracone and metacone, but without a metacingulum; (2) lower molars with mesiodistally compressed trigonids, a cristid obliqua that meets the trigonid buccal to the protocristid notch, a reduced metaconid, an enlarged paraconid, a carnassial notch, and paraconids and protoconids that are subequal in height; (3) as a result of those modifications, prevallum/postvallid shearing is reduced and the postvallum/prevallid shearing is emphasized; (4) enlarged upper and lower third premolars; and (5) three or fewer lower incisors (Fox and Naylor 2006; Scott and Fox 2015).

Specifically, we describe two dentary fossils of the genus *Eodelphis*, and we incorporate them and 20 other metatherian specimens into a biomechanical analysis based on beam theory (Therrien 2005). We use the resulting bending strength profiles to test whether *Eodelphis cutleri* and *Eodelphis browni*, like *D. vorax*, were capable of hard-object feeding (durophagy). We aim to improve our understanding of the evolutionary steps toward durophagy within the Stagodontidae and, more broadly, the diversification of feeding strategies within Metatheria during the Late Cretaceous.

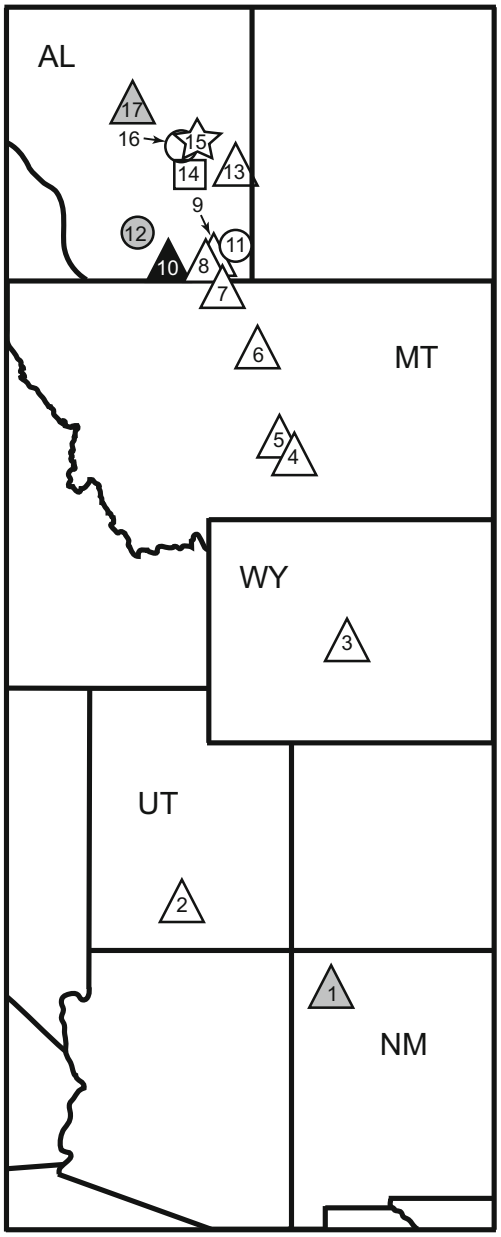

Background

The genus *Eodelphis* is represented in the fossil record by isolated teeth, dentary fragments with teeth, and cranial fragments from localities in the Western Interior of North America, most of them in Montana and Alberta (Fig. 1; Fox 1971; Sahni 1972; Rigby and Wolberg 1987; Eaton and Cifelli 1988; Fiorillo 1989; Montellano 1992; Peng and Russell 2001; DeMar and Breithaupt 2006; Scott and Fox 2015). These localities sample the Aquilan, Judithian, and possibly "Edmontonian" North American land mammal "ages" (NALMAs), which together correspond to a temporal range of ca. 84–70 million years ago (Ma) or late Santonian to early Maastrichtian of the Late Cretaceous (Cifelli et al. 2004; Wilson et al. 2010). Although the oldest specimen of this genus, referred to *Eodelphis* sp., was recovered from the Aquilan-age Deadhorse Coulee Member of the Milk River Formation in southern Alberta (Drees and Mhyr 1981; Fox and Naylor 2006), most specimens have been found at localities assigned a Judithian age (ca. 80–74 Ma; Wilson et al. 2010). Additionally, two very fragmentary dentaries that were recovered from Lane's Little Jaw Site Quarry in the Hell Creek Formation of southeastern Montana were tentatively assigned to *Eodelphis* (Kelly 2014). There is some uncertainty in the taxonomic identifications of the specimens and the age of the locality; it might be Lancian (latest Cretaceous), Puercan (earliest Paleocene), or mixed in age (Kelly 2014). Regardless, if the specimens are correctly assigned, the temporal range of *Eodelphis* would be extended at least ca. 4–5 Ma into the Lancian (Kelly 2014).

◀ **Fig. 1** Map of *Eodelphis* fossil localities in western United States and Canada. Circles for *E. cutleri*, squares for *E. browni*, the star for both *E. cutleri* and *E. browni*, and triangles for *Eodelphis* sp. 1 = Fossil Forest Quarry 1, Kirtland Fm., New Mexico; 2 = OMNH V5, Kaiparowits Fm., Utah; 3 = Fales Rocks/Barwin Quarry, Mesaverde Fm., Wyoming; 4 = Top Cat Quarry, Judith River Fm., Montana; 5 = Hidden Valley Quarry, Judith River Fm., Montana; 6 = Clambank Hollow Quarry, Judith River Fm., Montana; 7 = Coke's Microsite (UCMP V-82165), Makela's French 1 (UCMP V-77083), Put's Plunder (UCMP V-81234), and Makela's French 2 (UCMP V-77084), Judith River Fm., Montana; 8 = Hoodoo Site (RTMP L1126), Oldman Fm., Alberta; 9 = Pinhorn Range #1 (RTMP L1125), Foremost Fm., Alberta; 10 = Verdigris Coulee (UA-MR-6 and UA-MR-8), Milk River Fm., Alberta; 11 = Manyberries, Oldman Fm., Alberta; 12 = Scabby Butte Site 3, St. Mary Fm., Alberta; 13 = Dinosaur Provincial Park, Oldman Fm., Alberta; 14 = Sand Creek (middle fork, AMNH), Dinosaur Park Fm., Alberta; 15 = 6.4 m below mouth of Berry Creek (Little Sand Creek), Oldman Fm., Alberta; 16 = Onetree Creek, Oldman Fm., Alberta; 17 = 7 miles northwest of Rumsey, Edmonton Group, Alberta. Locality marker colors correspond to NALMA: black = Aquilan, white = Judithian, and gray = "Edmontonian" (Fox 1971; Sahni 1972; Rigby and Wolberg 1987; Eaton and Cifelli 1988; Fiorillo 1989; Montellano 1992; Peng and Russell 2001; DeMar and Breithaupt 2006; Scott and Fox 2015)

The two species of *Eodelphis* (*E. browni* and *E. cutleri*) were once proposed as sexual dimorphs of a single species by Montellano (1992), but Fox and Naylor (2006) convincingly argued that the qualitative differences in their dentition and inferred dietary preferences exceed what would be expected within a single species. Compared to *E. browni*, *E. cutleri* is larger, has a more robust dentary, more inflated teeth, and larger third premolars (Fox 1981; Scott and Fox 2015). Williamson et al. (2012, 2014) also treated *E. browni* and *E. cutleri* as separate species and recovered them as sister taxa within the Stagodontidae in their cladistic analyses of Late Cretaceous and Paleogene metatherians.

The genus *Didelphodon* is known from the Judithian through Lancian (early Campanian– late Maastrichtian; ca. 80–66 Ma) in the northern Western Interior of North America (Alberta, Saskatchewan, Montana, North Dakota, South Dakota, and Wyoming). The Lancian species, *D. vorax*, is known from across this geographic range from many specimens, including dentulous dentary fragments and partial crania (Wilson et al. 2016); a second Lancian species, *D. padanicus*, is restricted to only those specimens from South Dakota (Clemens 1966); and a third species, *D. coyi*, is known from only a few specimens from the "Edmontonian" and Lancian of Alberta (Fox and Naylor 1986, 2006). Several other poorly preserved specimens of *Didelphodon* from the Judithian Dinosaur Park Formation and the "Edmontonian" St. Mary River Formation, both in Alberta, have not been assigned to species (Sloan and Russell 1974; Fox and Naylor 1986; Scott and Fox 2015).

Both *Eodelphis* and *Didelphodon* have carnivorous dental adaptations, including the reduction of prevallum/postvallid shearing and emphasis of postvallum/prevallid shearing, but *Didelphodon* has more robust dental and dentary morphology, leading to the interpretation that it was more durophagous relative to *Eodelphis* and a powerful predator/scavenger (Clemens 1966, 1968; Scott and Fox 2015; Wilson et al. 2016). Furthermore, on the basis of size, premolar morphology, and stratigraphic occurrence, the conventional hypothesis is that *Didelphodon* arose from an *E. cutleri*-like ancestor (Clemens 1966; Fox and Naylor 1986, 2006; Scott and Fox 2015; but see Fox 1981; Fox and Naylor 1986 for comments on using morphological comparisons of premolars instead of molars). In contrast, Cohen (2017) hypothesized that the newly described Turonian stagodontid *Fumodelphodon* is more closely related to *Didelphodon* than *Eodelphis* is to *Didelphodon*, on the basis of similarities in premolar morphology and the results of his phylogenetic analysis. This would imply a ghost lineage that pre-dates the evolutionary split proposed by the conventional hypothesis. Additionally, the phylogenetic analysis results of Carneiro and Oliveira (2017) concluded that *Fumodelphodon* is most closely related to *Hoodootherium*; this clade (*Fumodelphodon* + *Hoodootherium*) is proposed as sister to a clade including (*Eodelphis* + [*Didelphodon* + *Eobrasilia*]). Nevertheless, we defer acceptance of the phylogenetic hypotheses of both Cohen (2017) and Carneiro and Oliveira (2017) until further evidence can be brought to bear on the association of the isolated premolars and molars referred to *Fumodelphodon*—presently, it is made primarily on the basis of size (Cohen 2017)—and on the proposed phylogenetic relationships between *Didelphodon* and *Fumodelphodon* and between *Didelphodon* and *Eobrasilia*. Because a detailed phylogenetic analysis of the Stagodontidae is beyond the scope of this paper, we proceed with the working hypothesis that *Didelphodon* arose from an *E. cutleri*-like ancestor (Clemens 1966; Fox and Naylor 1986, 2006; Scott and Fox 2015).

Accordingly, it might be expected that *E. cutleri* possessed morphology reflecting a trend toward durophagy, whereas *E. browni* would lack or have fewer of these adaptations. Indeed, the premolars of *E. cutleri*, like those of *Didelphodon*, are more robust than those of *E. browni* (Scott and Fox 2015). *Eodelphis cutleri* has thus been interpreted as having had a more scavenging or hard-object feeding habit, whereas *E. browni* has been interpreted as insectivorous or possibly carnivorous (Scott and Fox 2015). It follows that the feeding capabilities of these species should also be evident in the morphology of their dentaries; however, until now this hypothesis has not yet been quantitatively tested.

Institutional Abbreviations

AMNH, American Museum of Natural History, New York, New York, USA.; **MOR**, Museum of the Rockies, Bozeman, Montana, USA; **NHMUK**, Natural History Museum, United Kingdom, London, UK; **OMNH**, Oklahoma Museum of Natural History, Norman, Oklahoma, USA; **RSMP**,

Palaeontological Collections of the of the Royal Saskatchewan Museum, Regina, Saskatchewan, Canada; **TMDC**, Two Medicine Dinosaur Center, Bynum, Montana, USA; **TMP**, Royal Tyrrell Museum of Palaeontology, Drumheller, Alberta, Canada; **UALVP**, University of Alberta Laboratory for Vertebrate Paleontology, Edmonton, Alberta, Canada; **UCMP**, University of California Museum of Paleontology, Berkeley, California, USA; **UWBM**, University of Washington Burke Museum, Seattle, Washington, USA.

Systematic Paleontology

MAMMALIA Linnaeus, 1758
THERIA Parker and Haswell, 1897
METATHERIA Huxley, 1880
MARSUPIALIFORMES Vullo et al., 2009
STAGODONTIDAE Marsh, 1889
EODELPHIS Matthew, 1916

EODELPHIS cf. *E. BROWNI* Matthew, 1916
Fig. 2a–f

Holotype

AMNH 14169: parts of the left squamosal and left jugal, anterior region of right dentary, and an incomplete left dentary with i1–3, p1–3, m2–4, and m1 roots present (Matthew 1916). The holotype was found in the Dinosaur Park Formation (Judithian; Late Cretaceous in age) in southeastern Alberta, Canada.

Referred Specimens

MOR 739, an incomplete right dentary with m2–4 and the alveoli of p2, p3, and m1 (Fig. 2a–c); TMDC TA2008.3.2, an incomplete right dentary with m1–4, fragments of p2–3, alveoli for p1, and an incomplete alveolus for the canine (Fig. 2d–f).

Locality Data

MOR 739 was found at MOR locality JR-120 "Long Time Waiting" in the Judith River Formation of Watson Coulee in Hill County, Montana. For more information regarding this locality, qualified researchers should contact the Museum of the Rockies. TMDC 2008.3.2 was found in the Judith River Formation of Kennedy Coulee in Hill County, Montana. For more information regarding this locality, qualified researchers should contact the Two Medicine Dinosaur Center.

Description

MOR 739 is a moderately well-preserved; right dentary; it includes most of the horizontal ramus, the anteroventral margin of the coronoid process, and the anterior part of the masseteric fossa, as well as m2–4 and the alveoli for p2, p3, and m1 (Fig. 2a–c). Most of the symphysis and the alveoli for the lower incisors, canine, and p1 are not preserved.

The horizontal ramus is long and gracile relative to that of *Didelphodon*. It is dorsoventrally deepest ventral to the m4 (10.55 mm) and tapers anteriorly (Fig. 2a, b). A slight bony projection on the ventral margin below the p2–p3 embrasure and fracturing along the lateral margins suggest that the specimen might have experienced mediolateral compressive deformation. An ovoid mental foramen occurs ventral to the level of the p3 alveoli; a second one is not present, but this absence may be due to the lack of preservation of the dentary ventral to the p1 posterior alveolus (Fig. 2a). The anterior edge of the coronoid process has a vertical orientation posterior to m4, as described for other dentaries of *E. browni* (Fox 1981). The preserved parts of the masseteric fossa are deep. Its anterior border does not extend onto the horizontal ramus of the dentary, but it does extend near to the ventral margin of the dentary, where there is a prominent masseteric line (Fig. 2a).

Alveoli for the p1 are not present, but a diastema anterior to the p2 alveoli provides some information about spacing of p1 relative to more posterior premolars (Fig. 2c). The p2 alveoli are subequal in size and laterally compressed (although some compression may be due to post-mortem deformation). The p3 alveoli are directly posterior to the p2 posterior alveolus; they are also larger than those of p2 and less laterally compressed (Table 1). The m1 alveoli are partly obscured by sediment infilling, but they are directly posterior to the p3 posterior alveolus; this differs from *Didelphodon* in which the anterior alveolus of m1 is buccal to the posterior alveolus of p3 (Clemens 1966).

The molar row of MOR 739 is slightly oblique to the long axis of the horizontal ramus (Fig. 2c). The molar crowns are well preserved, although some cusp apices, particularly those of the protoconids, are chipped or slightly worn. The m2 trigonid is narrower than the talonid and mesiodistally shorter than it. The trigonid angle is acute. The paraconid is taller than the protoconid, although the latter has a broken apex (and was probably taller than the paraconid before breakage), and the metaconid is by far the smallest trigonid cusp, as is characteristic of stagodontids (Clemens 1966; Fox 1981; Scott and Fox 2015). The paracristid, which shows some wear, steeply descends from the apex of the paraconid forming a notch at the lingual base of the protoconid; additionally, a ridge juts out from the mesial aspect of the apex of the paraconid, and extends ventrally toward the base of the cusp. The precingulid extends buccoventrally from just below the middle of the paracristid to the base of the protoconid. In distal view, the

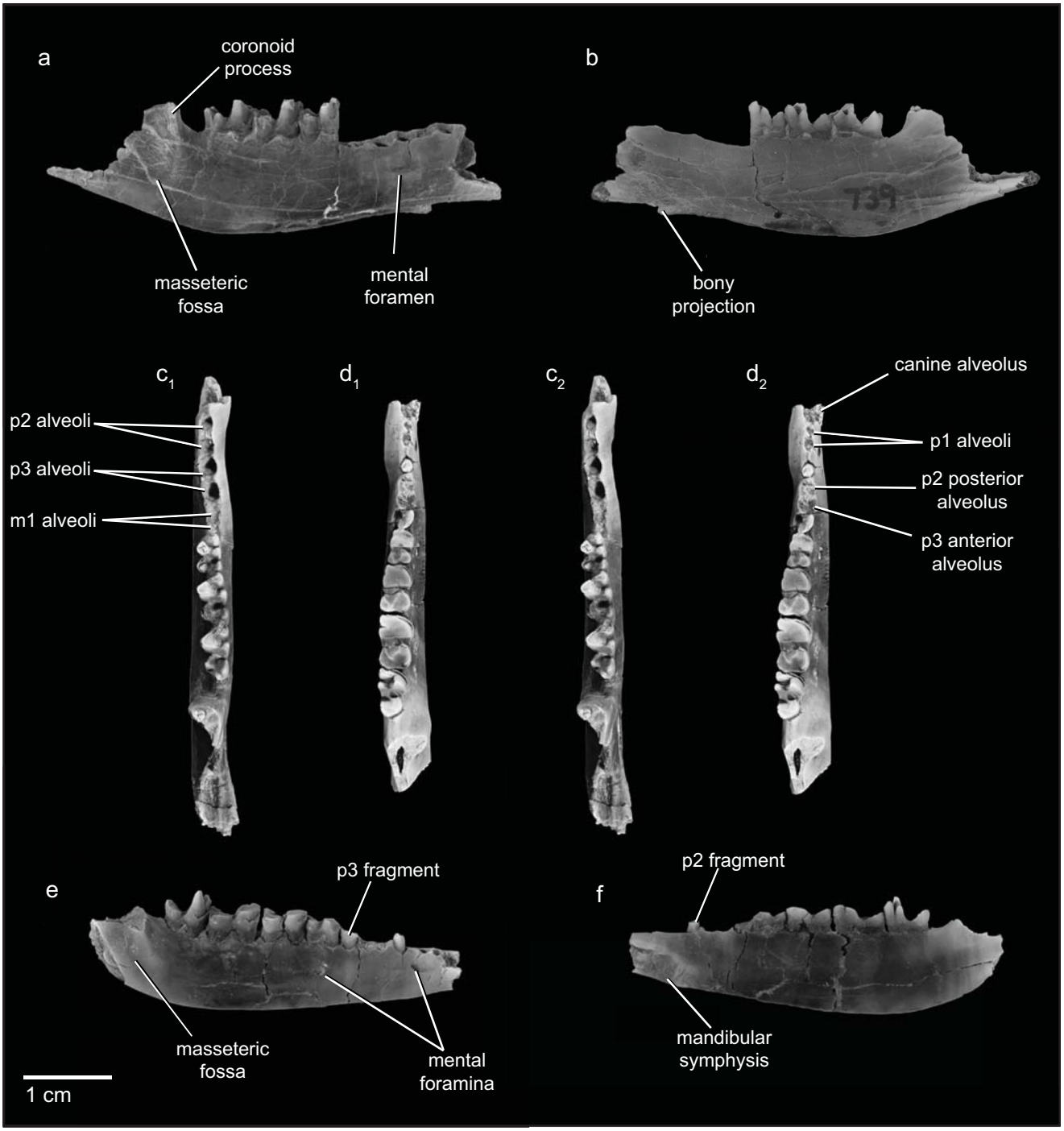

Fig. 2 MOR 739, an incomplete right dentary of *Eodelphis* cf. *E. browni* (**a**–**c**$_{1–2}$) TMDC TA2008.3.2, an incomplete right dentary of *Eodelphis* cf. *E. browni*, specimen (**d**$_{1–2}$–**f**). **a**, **e** buccal views; **b**, **f** lingual views; **c**$_{1–2}$, **d**$_{1–2}$ stereo occlusal views

protocristid is broad and V-shaped, rather than sharply notched; the lingual face of the trigonid is slightly convex; and the buccal and distal faces are nearly vertical. In occlusal view, the distal face is transverse, rather than oblique, to the mesiodistal axis of the crown. The talonid basin is broad and deepest mesiolingually. The entoconid and hypoconulid are "twinned" and taller than the hypoconid, although the hypoconid has a larger base. The entocristid, which shows some wear buccally, extends mesioventrally at a steep angle to make contact with the distal face of the trigonid at a sharp angle. The cristid obliqua extends from the hypoconid to contact the distal face of the trigonid buccal to the protocristid notch. Distally, the hypoconulid is braced between the precingulid and the mesial ridge of the paraconid of the m3, as seen in other specimens of *Eodelphis* and *Didelphodon* (e.g., Fox 1981).

Table 1 Measurements of lower premolar alveoli of *Eodelphis* cf. *E. browni*. Abbreviations: ant = anterior alveolus; L = length; post = posterior alveolus; W = width. All measurements in millimeters (mm)

	p1 alveoli		p2 alveoli		p3 alveoli	
	ant.	post.	ant.	post.	ant.	post.
MOR 739						
L	-	-	1.47	1.54	1.95	2.09
W	-	-	1.23	1.25	1.69	1.61
TMDC TA2008.3.2						
L	0.96	0.97	1.57	1.63	1.55	1.71
W	0.79	0.70	1.35	1.44	1.76	2.04

The m3 and m4 differ only slightly in morphology from the m2 (Fig. 2c). The m3 is larger than the m2 (Table 2), and the trigonid and talonid are subequal in length and width. The morphology and arrangement of the m3 trigonid cusps differ from those of the m2 in that the trigonid angle is more acute and the paraconid shows greater apical wear. The m3 talonid also differs from that of m2 in that the basin is deeper and the entoconid and hypoconulid show less wear. On m4, the trigonid is wider than the talonid. The entoconid and hypoconulid are of subequal height and almost as tall as the metaconid. All dental measurements are provided in Table 2.

TMDC TA2008.3.2 is a right dentary that preserves m1–4, fragments of p2 and p3, and alveoli for the p1 and canine (Fig. 2d–f). Overall, the dentary is like MOR 739, in having a gracile appearance compared to previously described specimens of *Didelphodon* and *E. cutleri*. It is deepest ventral to m4 (8.62 mm), and gently tapers in depth towards the canine. The anterior margin of the masseteric fossa is present, but the angular process, condyloid process, and most of the coronoid process are missing (Fig. 2e, f). The small portion of the anterior edge of the coronoid process that is preserved appears to steeply rise behind m4, as in MOR 739. At the anterior end, part of the symphysis is preserved, forming a roughened, raised, and oval surface (Fig. 2f). When the symphyseal region is oriented vertically, the anterior region of the dentary, the canine, and the premolars lean buccally—a condition that has also been observed in *Didelphodon* (Fig. 2d; Fox and Naylor 2006). There is an ovoid mental foramen ventral to m1, and another below the posterior alveolus of p1; this condition differs from that in MOR 739 in both the position and number of foramina, which may be due to individual variation (although see above for comments on non-preservation of the dentary ventral to the p1 posterior alveolus; Fig. 2e).

Table 2 Measurements of lower molars of *Eodelphis* cf. *E. browni*. Abbreviations: DW = distal width; L = length; MW = mesial width. All measurements in millimeters (mm)

	m1	m2	m3	m4
MOR 739				
L	-	4.21	5.22	6.27
MW	-	2.72	3.06	3.25
DW	-	2.80	3.00	2.68
TMDC TA2008.3.2				
L	3.90	5.00	5.64	5.10
MW	2.60	2.95	3.20	2.93
DW	2.52	3.17	3.43	2.33

The posterior half of a large canine alveolus is preserved. The p1 alveoli are ovoid, with the anterior one smaller and positioned slightly more buccally than the posterior one, as in the holotype of *E. browni* (Scott and Fox 2015). A slight diastema separates the posterior alveolus of p1 from the anterior alveolus of p2, as in MOR 739 (Fig. 2d).

The mesial root of p2 is preserved, but most of the crown and distal root are missing. The posterior alveolus of p2 is circular and is slightly larger than the anterior alveolus. The p3 alveoli are subequal in size and slightly larger than those of p2. The distal root of p3 and a fragment of the base of the crown are present, but the latter does not provide any coronal details. The mesial root of m1 is directly posterior to the distal root of p3, as in MOR 739 and other described specimens of *Eodelphis* (Fig. 2d; Clemens 1966).

The occlusal surfaces of m1–3 show substantial horizontal wear and exposed dentine, which prevent detailed description of the coronal morphology (Fig. 2d). The m4, in contrast, shows only slight apical wear on the trigonid cusps and along the paracristid and protocristid. The m4 protoconid is slightly taller than the paraconid, and the metaconid is the shortest and smallest of the trigonid cusps. These cusps form a more acute trigonid angle than what can be ascertained from the other molars. Some wear or damage on the talonid has made the individual cusps difficult to discern, although twinning of the entoconid and hypoconulid is evident (Fig. 2d). Overall, the minimal wear on m4 implies that this tooth erupted only shortly before death and the individual was a young adult. In contrast, the heavy wear on the m1–3 implies that this individual had a highly abrasive diet (Fox 1981) even before reaching dental maturity (eruption of m4). See Table 2 for dental measurements.

Remarks

The molar morphology (e.g., the small metaconid) of m2–m4 of MOR 739 and the m4 of TMDC TA2008.3.2, as well as the size of the molars and overall dentary morphology, support the referral of these specimens to the genus *Eodelphis*. Whereas molar morphology does not typically permit species-level identification of specimens of *Eodelphis*, premolar morphology, especially that of p3, is more diagnostic (Scott and Fox 2015). Specifically, (i) the p3 crown is generally larger, more inflated, and less sectorial in *E. cutleri* than in *E. browni* (Fox

1981; Scott and Fox 2015); (ii) the roots of p2 and p3 are parallel and vertically oriented in *E. cutleri*, but ventrally divergent in *E. browni* (Clemens 1966); and (iii) the premolars are aligned and relatively uncrowded in *E. browni*, but crowded in *E. cutleri* (Clemens 1966; Clemens, pers. comm. 2017). Computed tomography (CT) scans reveal that TMDC TA2008.3.2 and MOR 739 have p2 and p3 alveoli or roots that are vertical and parallel—the condition ascribed to both *E. cutleri* and *Didelphodon* (Online Resource 1; Clemens 1966). Both specimens described here have a small diastema between p1 and p2 (uncrowded), instead of having alveoli of successive premolars tightly packed (crowded) as seen in *E. cutleri* specimens (Clemens 1966: fig. 36); additionally, the p1 and p2 alveoli of TMDC TA2008.3.2 are mainly anteroposteriorly aligned with the horizontal ramus, not strongly oblique to it as in the holotype of *E. cutleri* (Clemens 1966; Scott and Fox 2015). Following a thorough cleaning of the holotype of *E. browni* (AMNH 14169), Scott and Fox (2015) noted that the p1 anterior alveolus of this taxon is also oriented obliquely across the dentary, in-line with the trajectory of the tooth row (contra Clemens 1966). Further study of the intra- and interspecific variation of these premolar characters in *Eodelphis* is required to confirm their reliability in taxonomic diagnoses. The morphology of p3 remains as the most consistent way to discriminate between the species of *Eodelphis*. However, because the p3 is not preserved in our specimens, we rely on premolar alignment, tooth measurements, and robustness of the dentary to tentatively refer them to *E. browni*.

The morphological differences between TMDC TA2008.3.2 and MOR 739 are likely due to some combination of intraspecific variation, ontogenetic stage, sexual dimorphism, and differences in feeding behavior of the individuals represented. Both specimens represent dentally mature individuals (fully erupted m4); however, the dentary and the teeth of MOR 739 are larger than those of TMDC TA2008.3.2 (Fig. 2; Tables 1 and 2), possibly reflecting sexual dimorphism, age, intraspecific variation, or some combination of those factors. Intriguingly, the molar wear pattern of MOR 739 runs counter to the interpretation that the larger individual is older. The m1–4 of MOR 739, the larger specimen, shows only minor apical wear and very little horizontal wear, in contrast to the pattern in TMDC TA2008.3.2, the smaller specimen. Extensive wear to m1–3 of TMDC TA2008.3.2 has formed a broad horizontal platform. The m4 is relatively unworn, suggesting that this tooth erupted only shortly before the individual died. This would imply that the individual was a young adult and that the extensive wear on m1–3 formed mostly during earlier ontogenetic stages. The m4 of MOR 739, the larger specimen, is relatively unworn as well, but no more so than its m1–3; thus, it probably represents an individual at a similar ontogenetic stage relative to TMDC TA2008.3.2. In their observations of dentulous dentary fragments of *Eodelphis*, Fox and Naylor (1995, 2006) inferred that juveniles of *Eodelphis* primarily employed molar shearing, and individuals shifted toward more crushing as wear leveled the cusps into broad platforms; this functional shift also implies a shift in diet. The molar wear patterns in our specimens imply that timing of this transition varies across individuals, such that some juveniles might have begun to emphasize crushing and hard-object feeding before dental maturity.

MOR 739 was found in deposits that include three stratigraphically distinct nesting horizons of the lambeosaurine dinosaur *Hypacrosaurus stebingeri* (Horner 1999). MOR 739 was found in the middle horizon of this stratigraphic sequence. Nest predation has been hypothesized as a factor in the extinction of non-avian dinosaurs (Benton 1990), and mammals have been proposed as possible predators of dinosaur eggs and hatchlings (e.g., Wilson et al. 2016; Bois and Mullin 2017). Bois and Mullin (2017) also suggested that Late Cretaceous mammals, including *Didelphodon vorax* (5.2 kg; Wilson et al. 2016), *Bubodens magnus* (5.25 kg; Wilson 1987), and *Vintana sertichi* (9 kg; Krause et al. 2014), were all large enough to prey upon dinosaur eggs and hatchlings (also see Wilson et al. 2016 for discussion of dinosaur predation by *D. vorax*). We speculate that *Eodelphis* also might have preyed upon or scavenged the hatchlings and eggs of *H. stebingeri*, given the carnivorous adaptations of its molars, in general, and the juxtaposition of MOR 739 and the lambeosaurine nests. Certainly, *Eodelphis* would have been capable of cracking eggs open with its jaws and teeth or possibly by other egg-breaking strategies employed by extant egg predators (see Bois and Mullin 2017).

Bending Force Analysis of Metatherian Dentaries

Methods

To further constrain the feeding behavior of stagodontids and other metatherians, we quantified the biomechanical properties of the dentary in a sample of taxa. Following the methods of Therrien (2005), we modeled the horizontal ramus of the dentary as an elliptical, solid beam (i.e., modeled as a cantilever in which the articular condyle is the fulcrum), and estimated the resistance of that beam to bending forces in the mediolateral and dorsoventral axes. A hollow beam model was not used because developing this model would require quantification of the cortical bone distribution in the horizontal ramus via CT scans of all specimens, and we did not have access to such data (Biknevicius and Ruff 1992a; Therrien et al. 2016). Although hollow beam models are more accurate in determining the exact values of bending strength along the dentary, Therrien et al. (2016) demonstrated that solid beam

and hollow beam models are generally consistent in their depiction of relative patterns of change in bending force along the dentary. Because we are interested in the relative patterns of bending force among taxa, the use of solid beam models is appropriate. The second moment of area, I, is a measure of the distribution of bone around a given axis (i.e., Ix = distribution of bone about the mediolateral axis; Iy = distribution of bone about the dorsoventral axis) and is used to calculate the bending force of the dentary about each axis (i.e., Zx = bending force about the mediolateral axis; Zy = bending force about the dorsoventral axis; see Therrien 2005 for a review). The maximum force that the horizontal ramus of the dentary can withstand at any point is calculated as a ratio of the bending force (Z) over the distance separating the point of interest from the articular condyle (L; the fulcrum). Relative bending force is calculated as a ratio of the bending force about the mediolateral axis (Zx) over the bending force about the dorsoventral axis (Zy) and reflects the overall shape of the horizontal ramus (Therrien 2005; Therrien et al. 2016).

We also assumed that the material properties of the dentary bone do not vary among these taxa and individuals (Biknevicius and Ruff 1992a; Therrien 2005; Therrien et al. 2016) and that the dentary is principally loaded in bending (Hylander 1979, 1981, 1984, 1985). We ignored other loading types at the symphyseal region because this region is more complex than the rest of the dentary, undergoes various types of stresses during the chewing cycle (Hylander 1981, 1984, 1985; Hylander et al. 1998; Ravosa and Hogue 2004), and is not preserved in most fossil specimens in our sample. As such, a dorsoventrally deep horizontal ramus is interpreted as better able to withstand forces in the dorsoventral axis, which largely result from bite forces exerted on food (Hylander 1979; Therrien 2005). A mediolaterally wide horizontal ramus is interpreted as better able to withstand forces in the mediolateral axis, which are associated with transverse or torsional stresses produced by struggling prey or feeding on hard-object foods (Hylander 1979; Therrien 2005). The ratio of the bending force in the dorsoventral direction to the bending force in the mediolateral direction is a product of the cross-sectional shape of the dentary, and in large part reflects adaptation to load directions related to feeding habits (Biknevicius and Ruff 1992a; Therrien 2005; Therrien et al. 2016). Additionally, bending force of the dentary tends to scale with body size, such that larger bodied animals can generally withstand higher bending forces than smaller bodied animals can (Therrien 2005).

To construct force profiles of the dentaries, we took digital images of specimens using a Canon 5DS camera (Canon 100 mm Macro EF IS USM Lens), mounted on a high precision P-51 Cam-Lift system (Dun, Inc.), in standardized dorsal and lateral views with the same scale bar. We took measurements on those images and on published figures of specimens using ImageJ (Rasband 1997–2016). We measured dorsoventral depth and mediolateral width at six positions along the horizontal ramus, following the interdental gap scheme of Wilson et al. (2016; Fig. 3); this scheme was adapted from Therrien (2005) for use on metatherians, which in most cases have a different dental formula than eutherians. To gauge the effect of our approach versus direct measurement of the specimen, we compared measurements taken on a digital image of a cast (*D. coyi* TMP 84.64.1, cataloged as UCMP 152395) to those taken directly on the cast with digital calipers. The difference in measurements was minimal and did not affect the bending strength estimates for this specimen. To minimize error that could be introduced into our measurements by using published figures, we verified the orientation of specimens in the figures; if the orientation was oblique to the dorsal or lateral view, we did not include the image in our dataset. For stereopair images (seven included specimens), we selected a dorsal view image, if one had little to no lateral rotation. The resulting dataset is based on 22 specimens representing at least four extinct families (stagodontids, alphadontids, pediomyids, deltatheriids), two extant families (didelphids, dasyurids), eight genera, and at least 11 species of metatherians, including the measurements of *D. vorax*, *Didelphis virginiana*, and *Sarcophilus harrisii* from Wilson et al. (2016; measurements in that study were taken on actual specimens using digital

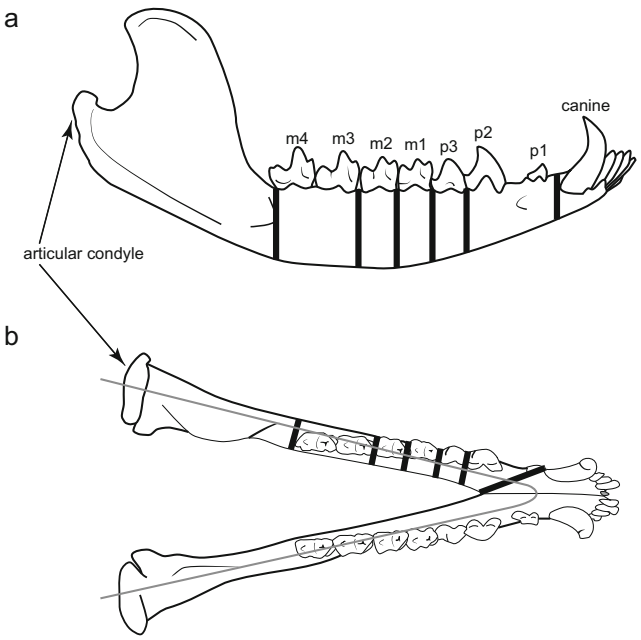

Fig. 3 Dorsoventral (**a**) and mediolateral (**b**) measurement scheme for bending strength analysis of metatherians dentaries following Therrien (2005) and Wilson et al. (2016). Measurements (thick lines) were taken at interdental gaps (canine, p2-p3, p3-m1, m1-m2, m2-m3, post m4) and perpendicular to the central axis of the dentary (gray line), except for the canine. The measurement at the canine was taken from the posterolingual aspect of the symphysis to the posterobuccal margin of the canine alveolus (Therrien 2005; Therrien et al. 2016). Specimen figured is UWBM 6640 (*Didelphis virginiana*)

calipers). See Online Resource 2 for details of the dataset (Fox 1979, 1981; Montellano 1988; Cifelli 1993; Fox and Naylor 2006; Fox et al. 2007; Scott and Fox 2015; Wilson et al. 2016) and Online Resource 3 for bending strength calculations.

Whereas *relative* bending forces (dorsoventral vs. mediolateral) can be assessed without a known distance of the interdental gap position to the articular condyle (Therrien 2005), estimates of the bending forces in a specific axis (dorsoventral or mediolateral) require that measurement. Because of the incomplete nature of the fossil record, a relatively complete dentary with the condyle is rarely preserved. Among specimens of *Eodelphis* used in this study, only the holotype of *E. browni* (AMNH 14169) preserves the articular condyle. Thus, for many specimens we were only able to estimate relative bending forces. To provide provisional estimates of the dorsoventral and mediolateral bending forces of the dentary of *E. cutleri* (a taxon critical to this study), we modeled the condyle position of the most complete *E. cutleri* specimen in this study (NHMUK M11532), first using a specimen of *E. browni* with an articular condyle as the model and second using a specimen of *D. vorax* with a condyle. The modeled condyle position of *E. cutleri* was calculated as follows:

$$L_{E.cutleri,\ i} = \frac{tooth\ row\ length_{E.cutleri} * L_{E.browni\ \text{or}\ D.vorax}}{tooth\ row\ length_{E.browni\ \text{or}\ D.vorax}},$$

where $L_{E.\ cutleri}$ is the modeled distance of the articular condyle to each interdental gap for *E. cutleri*, *i* represents the interdental gap position, $L_{E.\ browni\ \text{or}\ D.\ vorax}$ is the actual distance of the articular condyle to that interdental gap in *E. browni* or *D. vorax*, and tooth row length is length from the posterior part of the canine alveolus to the distal end of the m4. The resulting distances from both models were then used in calculations, which constrain the dorsoventral and mediolateral bending forces for *E. cutleri*.

Data Availability Statement All data generated or analyzed during this study are included in this published article [and its supplementary information files].

Results

The dorsoventral force profiles (Zx/L; Fig. 4a, d) of the metatherian dentaries studied here are characterized as either: (1) a relatively steep, positive slope posteriorly (*E. browni* and *E. cutleri*), in which bending force is low at the canine and increases toward the molars; (2) a positive slope posteriorly (*D. vorax* and *Didelphis virginiana*), in which bending force is not as low at the canine and gently increases toward the molars; or (3) an initially negative slope at the anterior region of the dentary that becomes positive posteriorly towards a maximum value behind m4 (*D. coyi* and *Sarcophilus harrisii*). These results are mostly consistent with the predictions that the dentary typically encounters the greatest forces, in either the dorsoventral or mediolateral directions, at the posteriormost position (post m4) due to the mechanical advantage of short output levers (i.e., the distance to the fulcrum, which is the articular condyle), and that larger bodied taxa can generate and withstand higher dorsoventral bending forces (i.e., bite forces) than smaller bodied taxa can (Fig. 4a, d). For example, dorsoventral bending force values increase with body size from *Alphadon halleyi* to *E. browni* to *Sarcophilus harrisii*.

The mediolateral force profiles (Zy/L; Fig. 4b, e) of the studied metatherian dentaries are characterized as either: (1) a relatively steep, positive slope posteriorly (*E. browni*), in which bending force of the dentary is low at the canine and increases toward the molars; (2) an initially negative slope at the anterior region of the dentary that becomes positive posteriorly toward a maximum value behind m4 (*D. coyi* and *E. cutleri*); or (3) a relatively flat profile (*D. vorax* and *Didelphis virginiana*) or a broad U-shaped curve (*Sarcophilus harrisii*), in which bending force of the dentary at the canine is subequal or greater than values at the molars. The relatively high Zy/L values anteriorly on the dentary of *E. cutleri* indicate that it was better able to withstand mediolateral forces at the canine (i.e., from torsional stresses or hard-object feeding) than the dentary of *E. browni* was (Fig. 4b).

The relative bending force (Zx/Zy) profiles (Figs. 4c, f and 5; Online Resource 4) are characterized as either: (1) a relatively steep, positive slope posteriorly, in which relative bending force at the molars is more than double the values at the anterior region of the dentary (*Turgidodon praesagus*, *Nanocuris improvida*, and *Didelphis virginiana*); a pattern that implies a sharp increase posteriorly in the capability of these dentaries to withstand dorsoventral loading (as reflected by horizontal ramus depth) relative to mediolateral loading (as reflected by horizontal ramus width); (2) a broad inverted U-shaped curve, in which relative bending force at the canine is subequal to 1.00, considerably less than values at the molars (*Kokopellia juddi*, *D. vorax*, *D. coyi*, *Sarcophilus harrisii*, and *E. cutleri*); a pattern that indicates the capability of some of these dentaries to withstand greater dorsoventral loading anteriorly (e.g., at the level of the crushing premolars and anterior molars) than would be expected by lever mechanics alone; or (3) a relatively flat line in which relative bending force at anterior region of the dentary is subequal to the values posteriorly at the molars (*E. browni*); a pattern that implies a consistent ratio of dorsoventral to mediolateral force along the horizontal ramus length, with the advantage in the dorsoventral direction. Note that the profiles of one specimen of *D. coyi* (Fig. 4c) and one specimen of *D. vorax* (Online Resource 4) differ from that of all other specimens of *Didelphodon* (Fig. 5b and Online Resource 4); the relative bending force of the dentary at the canine for these specimens is greater than 1.00, rather than less than 1.00. This discrepancy

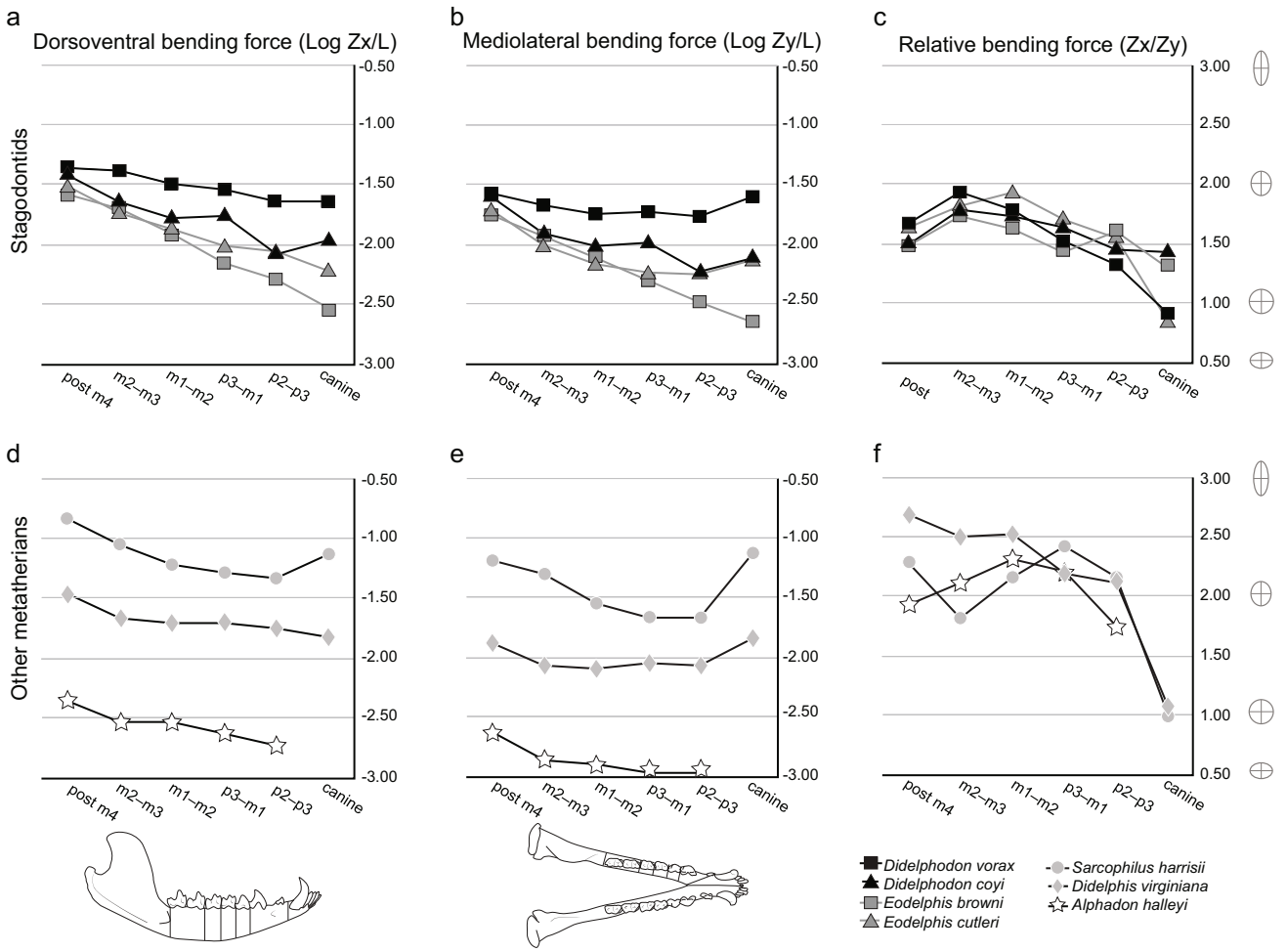

Fig. 4 Dorsoventral (**a**, **d**), mediolateral (**b**, **e**), and relative (**c**, **f**) bending force profiles of metatherian dentaries. Dentary cross-sections that correspond with relative bending force values are plotted in **c** and **f** (gray ovals with dorsoventral and mediolateral axes). **a–c**, stagodontid force profiles (black squares = *Didelphodon vorax* UWBM 102139; black triangles = *Didelphodon coyi* TMP 84.64.1; dark gray squares = *Eodelphis browni* AMNH 14169; dark gray triangles = *Eodelphis cutleri* NHMUK M11532 in **c**). In **a** and **b**, plotted values for *E. cutleri* are based on the *E. browni* model (see Methods section; the *D. vorax* model resulted in a similar profile). **d–f**, other metatherian force profiles (light gray circles = extant *Sarcophilus harrisii* UWBM 20671; light gray diamonds = extant *Didelphis virginiana* UWBM 12555; white stars = *Alphadon halleyi* MOR 250). Zx = section modulus or bending strength about the mediolateral axis; Zy = section modulus or bending strength about the dorsoventral axis; L = distance from the articular condyle (fulcrum of the cantilever) to each studied interdental gap (Therrien 2005)

implies that these individuals were not as well adapted for resisting mediolateral loads anteriorly (e.g., hard-object feeding) as other individuals of *Didelphodon* that we sampled—a result that might reflect ontogenetic variation in feeding behavior (Peng et al. 2017).

?*Protolambda clemensi* and *Alphadon halleyi* are represented by incomplete dentaries from which relative bending force at the canine could not be calculated. *Alphadon halleyi* has a broad, inverted U-shaped profile from the premolars to the molars, like that of *Didelphodon* (Fig. 4c, f). ?*Protolambda clemensi* is unique in our sample in having a gentle negative slope posteriorly (i.e., Zx/Zy of the premolars > Zx/Zy of the molars), implying that the dentary becomes relatively wider posteriorly. Nevertheless, because both *Alphadon halleyi* and ?*Protolambda clemensi* have relative bending force values greater than 1.00, each had a greater capacity to withstand dorsoventral loads, rather than mediolateral loads, along the dentary (Fig. 5a).

As for the specimens of *Eodelphis* described in this paper, the relative force profile of MOR 739 (*Eodelphis* cf. *E. browni*, see above in Systematic Paleontology) differs from all other specimens of *Eodelphis* and other metatherian taxa included in this study (Fig. 5b). It forms a broad U-shaped curve, in which the relative bending force value at the p2–p3 position is high (i.e., the dentary is over 2.5 times deeper than it is wide at this point in the dentary). The relative bending force values along the entire horizontal ramus are between 2.00 and 2.50—greater than the relative bending force values of other *Eodelphis* specimens (< 2.00). We interpret these anomalously high relative bending force values as being skewed toward dorsoventral loadings as a result of the post-mortem lateral compression experienced by MOR 739

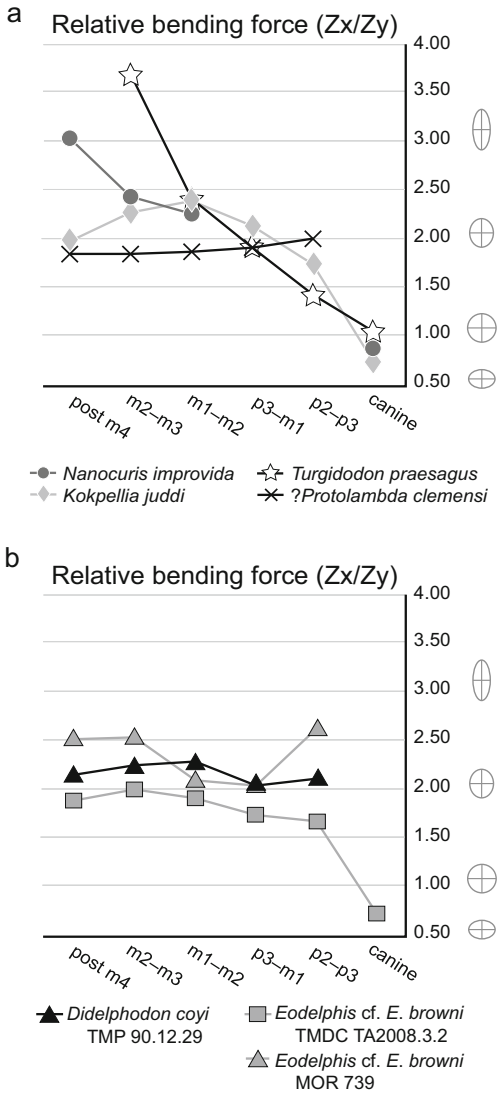

Fig. 5 Relative bending force profiles of additional metatherian dentaries. **a** non-stagodontid metatherians (gray circles = *Nanocuris improvida* RSM P2523.260; light gray diamonds = *Kokopellia juddi* OMNH 26361; white stars = *Turgidodon praesagus* UALVP 670; black Xs = ?*Protolambda clemensi* UALVP 14810) and **b** stagodontids (black triangles = *Didelphodon coyi* TMP 90.12.29; gray squares = *Eodelphis* cf. *E. browni* TMDC TA2008.3.2; gray triangles = *Eodelphis* cf. *E. browni* MOR 739). Dentary cross-sections that correspond with relative bending force values are plotted in **a** and **b** (gray ovals with dorsoventral and mediolateral axes)

(see Systematic Paleontology). For TMDC TA2008.3.2, despite gross morphological similarity to *E. browni*, it has a relative force profile of the dentary that is better aligned with that of *E. cutleri* (Figs. 4c and 5b). It forms a broad inverted U-shaped curve, in which relative bending force at the anterior region of the dentary is less than 1.00 (considerably lower than at the molars), as in *Didelphodon* and *E. cutleri*. Thus, anteriorly the dentary was better adapted to withstand forces in the mediolateral direction than in the dorsoventral direction. This profile could reflect intraspecific or ontogenetic variation, possibly resulting from a morphogenetic response to a more abrasive diet (recall the heavily worn m1–3; see Systematic Paleontology: Remarks).

The Evolution of Durophagy in the Stagodontidae

In this study, we examined dentary shape with the goal of inferring function and feeding behavior in extinct metatherians, particularly stagodontids. Whereas considerable research has shown how tooth shape correlates with function and diet in extant mammals (e.g., see review by Evans 2013), the link between dentary shape, function, and diet has not been as well established. In fact, Ross and Iriarte-Diaz (2014) remarked that most studies have not shown a clear relationship between dentary morphology and diet (e.g., Brown 1997; Daeling and Grine 2006; Wright et al. 2009); notably, those studies were mainly focused on primates, a group in which the form-function relationship might be complicated by the transverse movement permitted at the jaw joint. In contrast, carnivorans, which have little to no transverse movement at their jaw joint, have a stronger correlation between dentary morphology and feeding behavior (Therrien 2005; Therrien et al. 2016). The extant marsupials in our study, as well as the Cretaceous metatherians that are known by more complete fossils (e.g., *Didelphodon* and *Eodelphis*), have a jaw articulation that similarly did not permit much transverse movement (spool-shaped articular condyle that fits within a trough-like glenoid fossa). As such, we argue that inferring function and feeding behavior from the dentary morphology of these taxa should be tenable. Indeed, the bending force profiles of the two extant taxa in our sample, *Sarcophilus* and *Didelphis*, are consistent with their known feeding ecologies. Thus, we used the results of our bending force analysis to interpret functional and paleoecological changes within stagodontids and across Cretaceous metatherians.

Mediolateral Buttressing of the Dentary

The mediolateral force profile of *E. cutleri* is intermediate between that of *E. browni* and *D. vorax*. The mediolateral force values of the dentary of *E. browni* indicate that it was not able to withstand large torsional loads at the canine (Fig. 4b), such as those induced by struggling prey or by cracking hard objects; instead, it was better suited for dorsoventral loads, such as those incurred from large bite forces (Fig. 4c). Thus, *E. browni* likely preyed on insects and small vertebrates and was not capable of hard-object feeding (e.g., molluscs and bone). In contrast, the anterior region of the dentary of *E. cutleri* is mediolaterally buttressed (Fig. 4b). Although the associated mediolateral bending force values are less than those of *D. vorax*, they are subequal to those of *D. coyi* at both

the canine and p2–p3 positions (the profiles then diverge from each other posteriorly). It follows that the dentary of *E. cutleri* could have withstood relatively large torsional loads anteriorly, but critically it lacked the mediolateral buttressing more posteriorly to withstand similar loads at the p3 crushing locus and the molars. In contrast, both species of *Didelphodon* possessed this mediolateral buttressing posteriorly, suggesting a greater capacity for durophagous diets as compared to *E. cutleri*.

Dorsoventral Buttressing of the Dentary

The dorsoventral bending force values of the four stagodontid taxa included in this study are similar posteriorly (post m4 position) but differ anteriorly (Fig. 4a). In *E. browni*, which serves as a baseline, values are low anteriorly and steadily increase posteriorly as bite forces increase with decreasing distance to the fulcrum (i.e., the out lever becomes shorter). In comparison, the dorsoventral force profiles of *E. cutleri*, *D. coyi*, and *D. vorax* are increasingly shallower (in that order), reflecting increasingly greater bending force values at the anterior region of the dentary. This dorsoventral buttressing in the dentary of *E. cutleri* extends from the canine to the p2–p3 position; in *D. coyi*, it extends from the canine to the p3–m1 position; and in *D. vorax*, it extends the length of the dentary (canine to post m4 position) and the values are greater than in all other taxa. This pattern of dorsoventral buttressing implies that *E. cutleri* could have generated and withstood greater bite forces in the anterior region of the dentary than what *E. browni* could have, but less than what either species of *Didelphodon* could have. In *D. coyi*, the sharp uptick in dorsoventral bending force values at the p3–m1 position (and continuing more posteriorly in *D. vorax*) represents buttressing around the crushing locus, a feature that appears to be critical in hard-object feeding (Biknevicius and Ruff 1992a; Therrien 2005: Figs. 6 and 7). *Eodelphis cutleri* lacks this degree of dorsoventral buttressing, despite having a p3 that appears well suited for crushing (i.e., large, bulbous).

Thus, the results of our bending strength analysis support the hypothesis that *E. cutleri* was better suited for durophagy than *E. browni*, but less so than either species of *Didelphodon* (Fig. 4a–c). In *Didelphodon*, the dentary was buttressed anteriorly and at the crushing locus to withstand the high torsional stresses and the high bite forces involved in hard-object feeding. Hyaenids and *Sarcophilus harrisii* similarly exhibit both dorsoventral and mediolateral buttressing, suggesting that buttressing both axes might be required for mammals that consume a high percentage of hard-object foods (Therrien 2005: fig. 7). In turn, the lack of buttressing at the crushing locus (and posteriorly) of *E. cutleri* implies that its capacity for durophagy was less than that of *Didelphodon*, an interpretation that is consistent with other morphological differences between these taxa; for example, the cross-sectional shape of the canine of *E. cutleri* is not as round as that of *Didelphodon*, indicating that it would not have been as resistant to torsional stresses incurred when deep bites contacted bone or when adjacent premolars crushed hard objects (Wilson et al. 2016; fig. 6).

Vertical Position of the Articular Condyle of the Dentary

The relative vertical position (i.e., elevation) of the articular condyle differs between *Eodelphis* and *Didelphodon*, and likely affected their relative durophagous capabilities. The

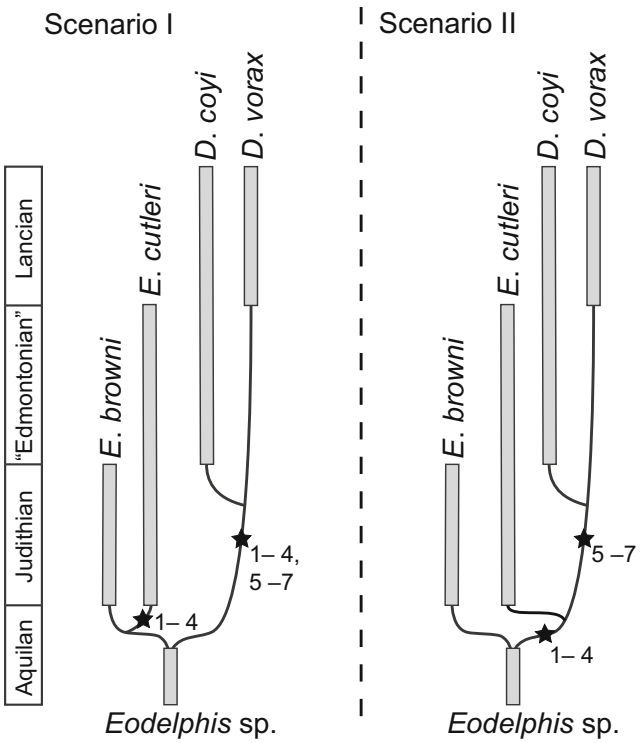

Fig. 6 Possible scenarios for the evolution of durophagy in the Stagodontidae. In Scenario I, the evolution of durophagy traits is mapped, using parsimony, on the accepted tree of stagodontids (Clemens 1966; Fox and Naylor 1986, 2006; Scott and Fox 2015). In Scenario II, the evolution of durophagy traits is mapped on a tree that was constructed to minimize independent the evolution of these traits in stagodontids. The morphological traits are: 1 = an enlarged, convex ultimate premolar (p3) for crushing; 2 = reduced length of the horizontal ramus (manifest as crowded premolars), resulting in increased mechanical advantage via shorter out levers; 3 = mediolateral buttressing of the anterior region of the dentary capable of withstanding greater torsional stresses; 4 = dorsoventral buttressing of the anterior region of the dentary capable of withstanding greater bite forces anteriorly; 5 = dorsoventral buttressing of the dentary posterior to premolars capable of withstanding greater bite forces associated with the crushing locus; 6 = rounded cross-sectional shape of the canines capable of withstanding stresses incurred from deep bites that contact hard objects such as bone or from adjacent premolars crushing objects; and 7 = lower position of the articular condyle relative to the tooth row. Gray bars represent the temporal range of fossil occurrences for each taxon. Black stars represent the evolution of the numbered morphological traits

articular condyle of *Eodelphis* is only preserved in anatomical position in the holotype of *E. browni* (AMNH 14169), where the vertical position of the articular condyle is dorsal to the level of the tooth row. In *Didelphodon*, it is more ventral, closer to the level of the tooth row. Such a difference in condyle position could impact the mechanical advantage of dentary rotation around a mediolaterally oriented axis (i.e., the pitch; Grossnickle 2017; Grossnickle pers. comm. 2017, 2018). Specifically, if we assume that (i) the axis of pitch rotation of the dentary passed through or near the articular condyles, (ii) the typical bite point (i.e., out-lever distance) does not differ significantly, and (iii) the relative coronoid height did not change substantially between these taxa, then the relatively lower articular condyle of *Didelphodon* would have moved the axis of rotation farther from the force vector of the temporalis muscle—most likely the largest and most powerful masticatory muscle of these mammals (Turnbull 1970)—and would have thus increased the length of the moment arm of the temporalis muscle and enabled the temporalis to generate more force during pitch (Maynard Smith and Savage 1959). Such mechanical advantage would have been beneficial for crushing hard objects, especially at more anterior regions of the dentary.

The vertical position of the articular condyle also modifies the effect of gape angle on bite force. Large gape angles increase the stretch of jaw muscles, and thereby decrease bite forces generated (Herring and Herring 1974; Lindauer et al. 1993; Turkawski and van Eijden 2001; Dumont and Herrel 2003; Santana 2016). However, a more ventral position of the articular condyle of the dentary would effectively result in a lower vertical position of the zygomatic arch and the pterygoid of the cranium, where the superficial masseter and the medial pterygoid muscles originate, respectively. It follows that those muscles, which insert on the angular process of the dentary, would experience less stretch during wide gapes, and, thus, associated bite forces would be less diminished (as long as the position of the angular process is unchanged; Herring and Herring 1974). Indeed, extant carnivores, which often require a wide gape for consumption of large prey, tend to have a vertically lower articular condyle and small angular process (Maynard Smith and Savage 1959; Grossnickle and Polly 2013). Accordingly, we infer that the more ventral position of the articular condyle of *Didelphodon* would have permitted it to maintain higher bite forces at wide gape angles to consume bigger, harder food items than *Eodelphis* could have.

Evolutionary Scenarios

Taken together, we propose two possible scenarios for the evolution of durophagy within the Stagodontidae (Fig. 6). If the sister-taxon relationship of *Didelphodon* and *Eodelphis* is valid (Scenario I), then our results would imply that a suite of morphological changes associated with durophagy evolved twice within stagodontids, once in *E. cutleri* and once in the most recent common ancestor of *D. coyi* and *D. vorax* (we exclude *D. padanicus* from the discussion because it was not included in our analyses). These changes would have included (1) development of an enlarged, inflated ultimate premolar (p3) for crushing; (2) the relative reduction of horizontal ramus length (manifest as crowded premolars; Clemens 1966), which resulted in increased mechanical advantage via shorter out levers; (3) mediolateral buttressing of the anterior region of the dentary to withstand greater torsional stresses; and (4) dorsoventral buttressing of the anterior region of the dentary to withstand greater bite forces anteriorly. Subsequently, the most recent common ancestor of *D. coyi* and *D. vorax* would have also evolved features 1–4 as well as three other features related to durophagy: (5) dorsoventral buttressing of the dentary posterior to premolars to withstand greater bite forces associated with the crushing locus (Clemens 1966; Therrien 2005; Wilson et al. 2016); (6) rounded cross-sectional shape of the canines for resisting stresses incurred from deep bites that contact bone or from adjacent premolars crushing objects (Wilson et al. 2016); and (7) a lower vertical position of the articular condyle to generate greater force during pitch rotation of the dentary. Scenario II is a more parsimonious alternative. Under this scenario, features 1–4 would have evolved only once in the most recent common ancestor of *E. cutleri* and *Didelphodon*; however, it would also imply that *Eodelphis* is paraphyletic, a topology that has not previously been supported by species-level cladistic analyses (Williamson et al. 2012, 2014). Features 5–7 would have then evolved in the most recent common ancestor of *D. coyi* and *D. vorax*, as in Scenario I. Additional morphological data are needed to resolve the phylogenetic relationships among species of *Eodelphis* and *Didelphodon* (as well as *Fumodelphodon* and *Hoodootherium*) and to further test these scenarios for the evolution of durophagy within the Stagodontidae.

Conclusions

In this study, we described two new dentary specimens of *Eodelphis*, and applied beam theory to a sample of 22 metatherian dentaries, an oft-neglected source of morphological data. The resulting bending strength profiles of the dentaries enabled us to investigate variation in the biomechanical capabilities of stagodontids and other metatherians. Our results point to two possible scenarios for the evolution of durophagy in stagodontids, one which requires considerable parallel evolutionary change within *Eodelphis* and *Didelphodon*, and the other which requires fewer evolutionary changes but a reconsideration of the monophyly of *Eodelphis*. Additional data and analyses will be required to discriminate between these two scenarios.

More broadly, our study highlights bending strength analysis of dentaries as a tool for constraining dietary inferences of extinct mammals independent of dental shape analyses (e.g., Evans 2013). Results from its novel application to a broad sample of fossil metatherians echo previous studies that have shown Mesozoic mammals were more ecomorphologically diverse than previously thought (e.g., Luo 2007; Wilson et al. 2012; Grossnickle and Polly 2013; Chen and Wilson 2015; Grossnickle and Newham 2016; Wilson et al. 2016). By way of example, the relative force profile of the mid-Cretaceous basal metatherian *Kokopellia juddi* is unexpectedly similar to those of taxa with durophagous capabilities (*Didelphodon*, *E*, *cutleri*, and *Sarcophilus harrisii*; Fig. 5a; Wilson et al. 2016). The relative force profile of the Campanian pediomyid ?*Protolambda clemensi*, in contrast, is unlike all other metatherian taxa included in this study—suggesting that posterior region of the dentary, rather than the anterior region, is better suited to withstand mediolateral loads. Furthermore, the relative force profile of the Lancian deltatheridiid *Nanocuris improvida* implies that this taxon was able to withstand high torsional stresses at the symphysis—such as those induced by struggling prey—corroborating previous interpretations of its carnivorous lifestyle (Fox et al. 2007; Wilson and Riedel 2010). In sum, this study has shed light on a broad range of morphologies of the dentary among Cretaceous metatherians that at minimum hint at a correspondingly broad range of biomechanical capabilities and feeding ecologies among these taxa, and that further study is merited.

Acknowledgments We thank the Museum of the Rockies (MOR), especially Dr. John Scannella, the University of California Museum of Paleontology (UCMP), especially Drs. Patricia Holroyd and William A. Clemens, and the Two Medicine Dinosaur Center Museum, especially Stacia Martineau and Cory Coverdell for access to specimens. We thank Dr. Sharlene Santana for access and use of the Santana Lab micro CT scanner, and Brody Hovatter for completing scans of these specimens. Funding for this research was provided by the National Science Foundation (NSF EAR SGP 1325674). We are grateful to members of the Wilson Lab (Dr. Stephanie Smith, Dr. Jonathan Calede, Dr. David DeMar, Jr., Lucas Weaver, and Brody Hovatter) for helpful comments and discussion concerning this manuscript. We also express our gratitude to Dr. David M. Grossnickle and one anonymous reviewer for their insightful comments and suggestions.

References

Benton MJ (1990) Scientific methodologies in collision: the history of the study of the extinction of the dinosaurs. Evol Biol 24:371–400

Biknevicius AR, Ruff CB (1992a) The structure of the mandibular corpus and its relationship to feeding behaviours in extant carnivorans. J Zool 228(3):479–507

Biknevicius AR, Ruff CB (1992b) Use of biplanar radiographs for estimating cross-sectional geometric properties of mandibles. Anat Rec 232(1):157–163

Binder WJ, Cervantes KS, Meachen JA (2016) Measures of relative dentary strength in Rancho La Brea *Smilodon fatalis* over time. PLoS One. https://doi.org/10.1371/journal.pone.0162270

Bois J, Mullin SJ (2017) Dinosaur nest ecology and predation during the Late Cretaceous: was there a relationship between Upper Cretaceous extinction and nesting behavior? Hist Biol. https://doi.org/10.1080/08912963.2016.1277423

Brown B (1997) Miocene hominoid mandibles: functional and phylogenetic perspectives. In: Begun DR, Ward CV, Rose MD (eds) Function, Phylogeny and Fossils: Miocene Hominoid Evolution and Adaptation. Plenum, New York, pp 153–171

Carneiro LM, Oliveira ÉV (2017) Systematic affinities of the extinct metatherian *Eobrasilia coutoi* Simpson, 1947, a South American early Eocene Stagodontidae: implications for "Eobrasiliinae." Rev Brasil Paleontol 20(3):355–372

Chen M, Wilson GP (2015) A multivariate approach to infer locomotor modes in Mesozoic mammals. Paleobiology 41(2):280–312

Cifelli RL (1993) Early Cretaceous mammals from North America and the evolution of marsupial dental characters. Proc Natl Acad Sci USA 90:9413–9316

Cifelli RL, Eaton JG (1987) Marsupial from the earliest Late Cretaceous of the western U.S. Nature 325:520–522

Cifelli RL, Eberle JJ, Lofgren DL, Lillegraven JA, Clemens WA (2004) Mammalian biochronology of the latest Cretaceous. In: Woodburne MO (ed) Late Cretaceous and Cenozoic Mammals of North America: Biostratigraphy and Geochronology. Columbia University Press, New York, pp 21–42

Clemens WA (1966) Fossil mammals of the type Lance Formation, Wyoming. Part II. Marsupialia. Univ Calif Publ Geol Sci 62:1–122

Clemens WA (1968) A mandible of *Didelphodon vorax* (Marsupialia, Mammalia). Los Angeles County Mus Nat Hist Contrib Sci 133:1–11

Cohen JE (2017) Earliest divergence of stagodontid (Mammalia: Marsupialiformes) feeding strategies from the Late Cretaceous (Turonian) of North America. J Mammal Evol. https://doi.org/10.1007/s10914-017-9382-0

Crompton AW, Kielan-Jaworowska Z (1978) Molar structure and occlusion in Cretaceous therian mammals. In: Butler PM, Joysey KA (eds) Studies on the Development, Structure, and Function of Teeth. Academic Press, New York, pp 249–287

Daeling DJ, Grine FE (2006) Mandibular biomechanics and the paleontological evidence for the evolution of human diet. In: Ungar PS (ed) Evolution of the Human Diet: The Known, the Unknown, and the Unknowable. Oxford University Press, Cary, pp 77–105

DeMar DG Jr, Breithaupt BH (2006) The nonmammalian vertebrate microfossil assemblages of the Mesaverde Formation (Upper Cretaceous, Campanian) of the Wind River and Bighorn basins, Wyoming. Bull New Mex Mus Nat Hist Sci 35:33–53

Drees NM, Mhyr DW (1981) The Upper Cretaceous Milk River and Lea Park formations in southeastern Alberta. Bull Canadian Petroleum Geol 29(1):42–74

Dumont ER, Herrel A (2003) The effects of gape angle and bite point on bite force in bats. J Exp Biol 206:2117–2123

Eaton JG, Cifelli RL (1988) Preliminary report on Late Cretaceous mammals of the Kaiparowits Plateau, southern Utah. Contrib Geol Univ Wyo 26(2):45–55

Evans AR (2013) Shape descriptors as ecometrics in dental ecology. Hystrix, Ital J Mammal. https://doi.org/10.4404/hystrix-24.1-6363

Fiorillo AR (1989) The vertebrate fauna from the Judith River Formation (Late Cretaceous) of Wheatland and Golden Valley counties, Montana. Mosasaur 4:127–142

Fox RC (1971) Marsupial mammals from the early Campanian Milk River Formation, Alberta, Canada. In: Kermack DM, Kermack KA (eds) Early Mammals. Suppl. No. 1, Zool J Linn Soc 50:145–164

Fox RC (1979) Mammals from the Upper Cretaceous Oldman Formation, Alberta. Can J Earth Sci 16:91–102

Fox RC (1981) Mammals form the Upper Cretaceous Oldman Formation. V. *Eodelphis* Matthew, and the evolution of Stagodontidae (Marsupialia). Can J Earth Sci 18:350–365

Fox RC, Naylor BG (1986) A new species of *Didelphodon* Marsh (Marsupialia) from the Upper Cretaceous of Alberta, Canada: paleobiology and phylogeny. Neues Jahrbuch für Geologie und Paläontologie Abhandlungen 172:357–380

Fox RC, Naylor BG (1995) The relationships of the Stagodontidae, primitive North American Late Cretaceous mammals. In: Sun A, Wang Y (eds) Sixth Symposium on Mesozoic Terrestrial Ecosystems and Biota. China Ocean Press, Beijing, pp 247–250

Fox RC, Naylor BG (2006) Stagodontid marsupials from the Late Cretaceous of Canada and their systematic and functional implications. Acta Palaeontol Pol 51(1):13–36

Fox RC, Scott C, Bryant HN (2007) A new, unusual therian mammal form the Upper Cretaceous of Saskatchewan, Canada. Cret Res 28: 821–829

Gill PG, Purnell MA, Crumpton N, Robson Brown K, Gostling NJ, Stampanoni M, Rayfield EM (2014) Dietary specializations and diversity in feeding ecology of the earliest stem mammals. Nature. https://doi.org/10.1038/nature13622

Grossnickle DM (2017) The evolutionary origin of jaw yaw in mammals. Sci Reports. https://doi.org/10.1038/srep45094

Grossnickle DM, Polly PD (2013) Mammal disparity decreases during the Cretaceous angiosperm radiation. Proc R Soc B 280:20132110. https://doi.org/10.1098/rspb.2013.2110

Grossnickle DM, Newham E (2016) Therian mammals experience an ecomorphological radiation during the Late Cretaceous and selective extinction at the K–Pg boundary. Proc R Soc B 283:20160256. https://doi.org/10.1098/rspb.2016.0256

Herring SW, Herring SE (1974) The superficial masseter and gape in mammals. Am Nat 108(962):561–576

Horner J (1999) Egg clutches and embryos of two hadrosaurian dinosaurs. J Vertebr Paleontol 19(4):607–611

Hylander WL (1979) The functional significance of primate mandibular form. J Morphol 160:223–240

Hylander WL (1981) Patterns of stress and strain in the macaque mandible. In: Carlson DS (ed) Craniofacial Biology, Monograph 10, Craniofacial Growth Series: Center for Human Growth and Development. University of Michigan, Ann Arbor, pp 1–35

Hylander WL (1984) Stress and strain in the mandibular symphysis of primates: a test of competing hypotheses. Am J Phys Anthropol 64: 1–46

Hylander WL (1985) Mandibular function and biomechanical stress and scaling. Am Zool 25:315–330

Hylander WL, Ravosa MJ, Ross CF, Johnson KR (1998) Mandibular corpus strain in primates: further evidence for a functional link between symphyseal fusion and jaw-adductor muscle force. Am J Phys Anthropol 107:257–271

Jernvall J, Hunter JP, Fortelius M (1996) Molar tooth diversity, disparity, and ecology in Cenozoic ungulate radiations. Science 274(5292): 1489–1492

Kelly TS (2014) Preliminary report on the mammals from Lane's Little Jaw Site Quarry: a latest Cretaceous (earliest Puercan?) local fauna, Hell Creek Formation, southeastern Montana. Paludicola 10(1):50–91

Kielan-Jaworowska Z-X, Cifelli RL, Luo ZX (2004) Mammals from the Age of Dinosaurs: Origins, Evolution, and Structure. Columbia University Press, New York

Krause DW, Hoffmann S, Wible JR, Kirk EC, Schultz JR, von Koenigswald W, Groenke JR, Rossie JB, O'Connor PM, Seiffert ER, Dumont ER, Holloway WL, Rogers RR, Rahantarisoa LJ, Kemp AD, Andriamialison H (2014) First cranial remains of a gondwanatherian mammal reveal remarkable mosaicism. Nature 515:512–517

Lindauer SJ, Gay T, Rendell J (1993) Effect of jaw opening on masticatory muscle EMG-force characteristics. J Dental Res 72:51–55

Luo Z-X (2007) Transformation and diversification in early mammal evolution. Nature 450:1011–1019

Matthew WD (1916) A marsupial from the Belly River Cretaceous. With critical observations upon the affinities of the Cretaceous mammals. Bull Am Mus Nat Hist 35:477–500

Maynard Smith J, Savage RJG (1959) The mechanics of mammalian jaws. School Sci Rev 40:289–301

Montellano M (1988) *Alphadon halleyi* (Didelphidae, Marsupialia) from the Two Medicine Formation (Late Cretaceous, Judithian) of Montana. J Vertebr Paleontol 8(4):378–382

Montellano M (1992) Mammalian fauna of the Judith River Formation (Late Cretaceous, Judithian), northcentral Montana. Univ Calif Publ Geol Sci 136:1–115

Peng A, Toews N, Wilson GP (2017) An ontogenetic investigation of a Cretaceous North American mammal, *Didelphodon vorax* (Metatheria: Marsupialiformes: Stagodontidae), through quantitative and descriptive analysis of the dentary. Geol Soc Am Annual Meeting Abstracts with Programs 49(6). https://doi.org/10.1130/abs/2017AM-300648

Peng J, Russell AP (2001) Vertebrate microsite assemblages (exclusive of mammals) from the Foremost and Oldman formations of the Judith River Group (Campanian) of southeastern Alberta: an illustrated guide. Provincial Museum of Alberta, Nat Hist Occas Pap 25:1–54

Rasband WS (1997–2016) ImageJ, U. S. National Institutes of Health, Bethesda, Maryland, https://imagej.nih.gov/ij/

Ravosa MJ, Hogue AS (2004) Function and fusion of the mandibular symphysis in mammals: a comparative and experimental perspective. In: Ross CF, Kay RF (eds) Anthropoid Origins: New Visions. Spinger Science+Business Media, LLC, New York, pp 413–462

Rigby JK, Wolberg DL (1987) The therian mammalian fauna (Campanian) of Quarry 1, Fossil Forest study area, San Juan Basin, New Mexico. Geol Soc Am Spec Pap 209:51–79

Ross CF, Iriarte-Diaz J (2014) What does feeding system morphology tell us about feeding? Evol Anthropol 23:105–120

Rougier GW, Davis BM, Novacek MJ (2015) A deltatheroidan mammal from the Upper Cretaceous Baynshiree Formation, eastern Mongolia. Cret Res 52:167–177

Rougier GW, Wible JR, Novacek MJ (1998) Implications of *Deltatheridium* specimens for early marsupial history. Nature 396: 459–463

Rougier GW, Wible JR, Novacek MJ (2004) New specimen of *Deltatheroides cretacicus* (Metatheria, Deltatheroida) from the Late Cretaceous of Mongolia. Bull Carnegie Mus Nat Hist 36: 245–266

Sahni A (1972) The vertebrate fauna of the Judith River Formation, Montana. Bull Am Mus Nat Hist 147:321–412

Sánchez-Villagra MR (2013) Why are there fewer marsupials than placentals? On the relevance of geography and physiology to evolutionary patterns of mammalian diversity and disparity. J Mammal Evol 20:279–290

Santana SE (2016) Quantifying the effect of gape and morphology on bite force: biomechanical modelling and in vivo measurements in bats. Funct Ecol 30:557–565

Scott CS, Fox RC (2015) Review of Stagodontidae (Mammalia, Marsupialia) from the Judithian (Late Cretaceous) Belly River Group of southeastern Alberta, Canada. Can J Earth Sci 52:682–695

Sloan RE, Russell LS (1974) Mammals from the St. Mary River Formation (Cretaceous) of southwestern Alberta. Life Sci Contrib R Ont Mus 95:1–21

Therrien F (2005) Mandibular force profiles of extant carnivorans and implications for the feeding behavior of extinct predators. J Zool 267:249–270

Therrien F, Quinney A, Tanaka K, Zelenitsky DA (2016) Accuracy of mandibular force profiles for bite force estimation and feeding behavior reconstruction in extant and extinct carnivorans. J Exp Biol 291:3738–3749

Turkawski SJJ, van Eijden T (2001) Mechanical properties of single motor units in the rabbit masseter muscle as a function of jaw position. Exp Brain Res 138:153–162

Turnbull WD (1970) Mammalian masticatory apparatus. Fieldiana: Geol 18:149–156

Williamson TE, Brusatte SL, Carr TD, Weil A, Standhardt BR (2012) The phylogeny and evolution of Cretaceous-Paleogene metatherians: cladistic analysis and description of new early Palaeocene specimens form the Nacimiento Formation, New Mexico. J Sys Palaeontol 10(4):635–651

Williamson TE, Brusatte SL, Wilson GP (2014) The origin and early evolution of metatherian mammals: the Cretaceous record. ZooKeys 465:1–76

Wilson GP (2013) Mammals across the K/Pg boundary in northeastern Montana, U.S.A.: dental morphology and body-size patterns reveal extinction selectivity and immigrant-fueled ecospace filling. Paleobiology 39(3):429–469

Wilson GP, Dechesne M, Anderson IR (2010) New latest Cretaceous mammals from northeastern Colorado with biochronologic and biogeographic implications. J Vertebr Paleontol 30(2):499–520

Wilson GP, Ekdale EG, Hoganson JW, Calede JJ, Vander Linden A (2016) A large carnivorous mammal from the Late Cretaceous and the North American origin of marsupials. Nat Comm. https://doi.org/10.1038/ncomms13734

Wilson GP, Evans AR, Corfe IJ, Smits PD, Fortelius M, Jernvall, J (2012) Adaptive radiation of multituberculate mammals before the extinction of dinosaurs. Nature 483:457–460

Wilson GP, Riedel JA (2010) New specimen reveals deltatheroidan affinities of the North American Late Cretaceous mammal *Nanocuris*. J Vertebr Paleontol 30(3):872–884

Wilson RW (1987) Late Cretaceous (Fox Hills) multituberculates from the Red Owl local fauna of western South Dakota. Dakoterra 3:118–122

Wright BW, Wright KA, Chalk J, Verderane MP, Fragaszy D, Visalberghi E, Izar P, Ottoni EB, Constantino P, Vinyard C (2009) Fallback foraging as a way of life: using dietary toughness to compare the fallback signal among capuchins and implications for interpreting morphological variation. Am J Phys Anthropol 140:687–699